PBRM1 Inactivation Promotes Upregulation of Human Endogenous Retroviruses in a HIF-Dependent Manner

Mi Zhou[1], Janet Y. Leung[1], Kathryn H. Gessner[1,2], Austin J. Hepperla[1,3], Jeremy M. Simon[1,3,4], Ian J. Davis[1,4,5], and William Y. Kim[1,4,6,7]

ABSTRACT

Clear cell renal cell carcinoma (ccRCC) is considered an immunotherapy-responsive disease; however, the reasons for this remain unclear. Studies have variably implicated *PBRM1* mutations as a predictive biomarker of immune checkpoint blockade (ICB) response, and separate studies demonstrate that expression of human endogenous retroviruses (hERV) might be an important class of tumor-associated antigens. We sought to understand whether specific mutations were associated with hERV expression. Two large, annotated genomic datasets, TCGA KIRC and IMmotion150, were used to correlate mutations and hERV expression. PBRM1 mutations were consistently associated with increased hERV expression in primary tumors. *In vitro* silencing of PBRM1, HIF1A, and HIF2A followed by RNA sequencing was performed in UMRC2 cells, confirming that PBRM1 regulates hERVs in a HIF1α- and HIF2α-dependent manner and that hERVs of the HERVERI superfamily are enriched in PBRM1-regulated hERVs. Our results uncover a role for PBRM1 in the negative regulation of hERVs in ccRCC. Moreover, the HIF-dependent nature of hERV expression explains the previously reported ccRCC-specific clinical associations of *PBRM1*-mutant ccRCC with both a good prognosis as well as improved clinical outcomes to ICB.

See related Spotlight by Labaki et al., p. 274.

Introduction

Renal cell carcinoma is a common cancer with 76,080 new cases diagnosed and 13,780 deaths in the United States in 2021 (1). Clear cell renal cell carcinoma (ccRCC) is the most common histologic subtype and has been genomically characterized by multiple groups, including The Cancer Genome Atlas (TCGA; ref. 2). ccRCC is associated with several recurrent genomic alterations, including a high rate of inactivation of the von Hippel-Lindau tumor suppressor gene, *VHL*, as well as other genes located on chromosome 3p: *PBRM1*, *SETD2*, and *BAP1* (2). *PBRM1*, the second-most frequently mutated gene in ccRCC (2), encodes a component of the polybromo BRG1-associated factor (PBAF) SWI/SNF chromatin remodeling complex, which plays key roles in nucleosome positioning and transcriptional regulation (3, 4).

It has been variably reported that *PBRM1* mutations are associated with improved clinical outcome and response to immune checkpoint blockade (ICB) in patients with metastatic ccRCC. Whereas original observations and follow-up studies demonstrate a correlation between *PBRM1* loss-of-function (LOF) mutations and second-line (VEGF TKI refractory), single-agent ICB response (5–7), other studies examining first-line, treatment-naïve cohorts treated with dual VEGF and ICB did not see this association (8, 9). In addition, evaluation of real-world datasets shows that although *PBRM1* mutations associate with ICB response in ccRCC (10), this does not hold up across other cancer types (11). Therefore, a better understanding of the mechanisms underlying the potential association between *PBRM1* mutations and ICB response might allow us to decipher these seemingly conflicting data.

Human endogenous retroviruses (hERV) are endogenous viral elements in the human genome derived from retroviruses (12). hERVs make up a substantial portion of the retroelements that comprise up to 8% of the human genome (13). It has been shown that hERV expression products can act as pathogen-associated molecular patterns (PAMP) to trigger innate immune responses (14) or provide antigenic epitopes stimulating adaptive immune responses (15). Multiple studies have identified altered expression of specific hERVs in many cancer types, including melanoma, breast cancer, and renal carcinomas (15–19). Recent studies also associate hERV expression with survival and response to ICB in ccRCC (15, 19). However, none of these studies examined the mechanisms by which hERVs are regulated in ccRCC.

We asked whether hERV expression is associated with ccRCC genomic alterations and found across multiple datasets that ccRCC tumors with *PBRM1* mutations have significant alterations in hERV expression. In particular, members of the HERVERI family are upregulated in *PBRM1*-mutant tumors. *In vitro* knockdown (KD) of *PBRM1* resulted in altered hERV expression in tumor cells, and these hERVs are enriched in HERVERI superfamily members. Moreover, the majority of PBRM1-induced changes in hERV expression are dependent on HIF1α and HIF2α. In aggregate, these results uncover a novel mechanism of hERV regulation in ccRCC and may underlie the clinical observations that *PBRM1*-mutant ccRCC have an improved prognosis and ICB response.

[1]Lineberger Comprehensive Cancer Center, University of North Carolina, Chapel Hill, North Carolina. [2]Department of Urology, University of North Carolina at Chapel Hill, Chapel Hill, North Carolina. [3]UNC Neuroscience Center, University of North Carolina at Chapel Hill, Chapel Hill, North Carolina. [4]Department of Genetics, University of North Carolina at Chapel Hill, Chapel Hill, North Carolina. [5]Department of Pediatrics, University of North Carolina at Chapel Hill, Chapel Hill, North Carolina. [6]Department of Pharmacology, University of North Carolina at Chapel Hill, Chapel Hill, North Carolina. [7]Division of Oncology, Department of Medicine, University of North Carolina at Chapel Hill, Chapel Hill, North Carolina.

Note: Supplementary data for this article are available at Cancer Immunology Research Online (http://cancerimmunolres.aacrjournals.org/).

Corresponding Author: William Y. Kim, Lineberger Comprehensive Cancer Center, University of North Carolina, CB# 7295, Chapel Hill, NC 27599-7295. Phone: 919-966-4765; Fax: 919-966-8212; E-mail: wykim@med.unc.edu

Cancer Immunol Res 2022;10:285–90

doi: 10.1158/2326-6066.CIR-21-0480

Materials and Methods

Data source

TCGA KIRC HERV expression matrix was requested from Smith and colleagues (15) Gene Mutation annotation was obtained from FireBrowse (http://firebrowse.org/#). RNA-sequencing (RNA-seq) data and mutation annotation of IMmotion150 cohort was downloaded from (EGAD00001004183) (20). RNA-seq from A704 cells was obtained from Gao and colleagues (21).

Quantification of HERV expression

The alignment and quantification of HERV expression was processed using the hervQuant workflow (15) from RNA-seq FASTQ files. Raw expression matrices were normalized using RPM and $\log_2$ transformed. hERVs with $\log_2$ expression <0.1 were filtered out as low-expressed hERVs.

Differential expression analysis

Differential expression analysis was performed using R package edgeR (v3.28.1) and limma (v3.42.2). Univariable logistic regression between *PBRM1* mutation and hERV expression was performed using R package stats (v3.6.2). Enrichment of hERVs was tested using χ^2 test. PBRM1-truncated mutations indicate frameshift and nonsense mutations only. Differential hERV expression from UMRC2 cells was controlled for FDR using the Benjamini–Hochberg method.

Cell culture and short hairpin RNA

All cells were short tandem repeat tested within 1 year of their use in these experiments. All cells were tested routinely for *Mycoplasma* every 2 months while in culture. All cells were cultured in DMEM (Sigma) supplemented with 10% FBS (Gibco) and maintained at 37°C at 5% CO_2. UMRC2 cells were obtained from Sigma Aldrich (catalog no. 08090511) in 2017. 293T cells were a gift from William G. Kaelin Jr. (Dana-Farber Cancer Institute, Harvard Medical School) in 2005. Cells with passage less than 50 passages were utilized for all experiments. PBRM1 KD was performed using an empty pLKO.1 vector (control) or pLKO.1 vector containing shRNA to human PBRM1 (TRCN0000015994, Thermo Fisher Scientific). Sequence CCGGCCGGAGTCTTTGATCTACAAACTCGAGTTTGTAGATC-AAAGACTCCGGTTTT pLKO.1 empty or pLKO.1-shPBRM1 lentivirus was generated by transfection of 293T cells with the above plasmids using Fugene6 transfection reagent (Promega, catalog no. E2691). UMUC2 cells were transduced with unconcentrated lentiviral supernatant and selected for infection using 3 μg/mL of puromycin.

The siRNA sequences to HIF1A and HIF2A are as follows. All siRNA were obtained from Ambion.

siHIF1–1 (Catalog: 4390824) Assay ID #s6539, human HIF1A
Sense: CCAUAUAGAGAUACUCAAATT
Antisense: UUUGAGUAUCUCUAUAUGGTG

siHIF1–2 (Catalog: 4390824) Assay ID #s4699, human HIF1A
Sense: CAAUAGCCCUGAAGACUAUTT
Antisense: AUAGUCUUCAGGGCUAUUGGG 1–2

siHIF2–1 (Catalog: 4390824) Assay ID #s4698, human EPAS1
Sense: CACCUACUGUGAUGACAGATT
Antisense: UCUGUCAUCACAGUAGGUGAA

siHIF2–2 (Catalog: 4390824) Assay ID #s6541, human EPAS1
Sense: CCUCAGUGUGGGUAUAAGATT
Antisense: UCUUAUACCCACACUGAGGTT

200 pmol of each siRNA was used for transfected into a 6-cm plate of target cells using Lipofectamine RNAiMAX transfection reagent (catalog no. 13778075).

UMRC2 RNA-seq data

RNA was extracted using Qiagen RNeasy Plus Mini kit (catalog no. 74134). RNA-seq libraries were prepared using TruSeq Stranded mRNA Library Preparation Kit (Illumina, catalog no. 20020595) according to the manufacturer's protocol. 75b paired-end reads were sequenced on Nextseq 500 (Illumina). Quality control–passed reads were aligned, quantified, and normalized using hervQuant workflow to generate the hERV expression matrix and followed by differential expression analysis.

Statistical analysis

General linear model using the R stats package was used for all univariable regressions. Differential hERV expression was calculated using the R edgeR and limma packages. Categorical enrichment tests were compared using χ^2 test.

Data availability

UMRC2 RNA-seq FASTQ files and hERV expression table are publicly available at GEO (Gene Expression Omnibus) under accession GSE176053.

Results

PBRM1 mutations correlate with increased hERV expression in primary ccRCC tumors

We first asked whether hERV expression was associated with ccRCC genomic alterations. To this end, we obtained hERV expression from 449 TCGA KIRC samples using the hervQuant analysis workflow (15). After filtering out lowly expressed hERVs, 1,680 hERVs were evaluated for association between their expression and the mutation status of significantly mutated genes in ccRCC as defined by the TCGA KIRC project. Specifically, we performed univariable logistic regression of individual hERV expression by gene mutation status [wild-type (WT), mutated; **Fig. 1A**]. *VHL*, *PBRM1*, and *BAP1* demonstrated strong positive association with the expression of a majority of hERVs. The positive association of *PBRM1* mutation with hERV expression was maintained even when restricted to *PBRM1* mutations predicted to cause LOF, that is, frameshift and nonsense (**Fig. 1A**). In contrast, mutations in *SETD2* and *MTOR* were negatively correlated with hERV expression. To assess whether tumor purity accounted for the association between gene mutation status and hERV expression, we correlated ESTIMATE scores from TCGA as the measure of stromal content (22) to expression of each individual hERV (Supplementary Fig. S1A) and found that the majority of hERVs had weak correlation to tumor purity. In addition, we found no significant difference of tumor ESTIMATE score between *PBRM1*-mutated and WT samples (Supplementary Fig. S1B). In aggregate, these results suggest the associations between gene mutation and hERV expression is not confounded by tumor purity.

We next evaluated a second cohort of 262 primary RCC tumors from IMmotion150 (20), which investigated the clinical activity of atezolizumab with and without bevacizumab versus sunitinib in patients with ccRCC (20). RNA-seq data were used to quantify hERV expression by hervQuant (15) as described for the TCGA KIRC samples above. Application of the same filtering and transformation parameters resulted in 1,434 hERVs for downstream analysis. The expressed hERVs detected in the two datasets were similar, with 87%

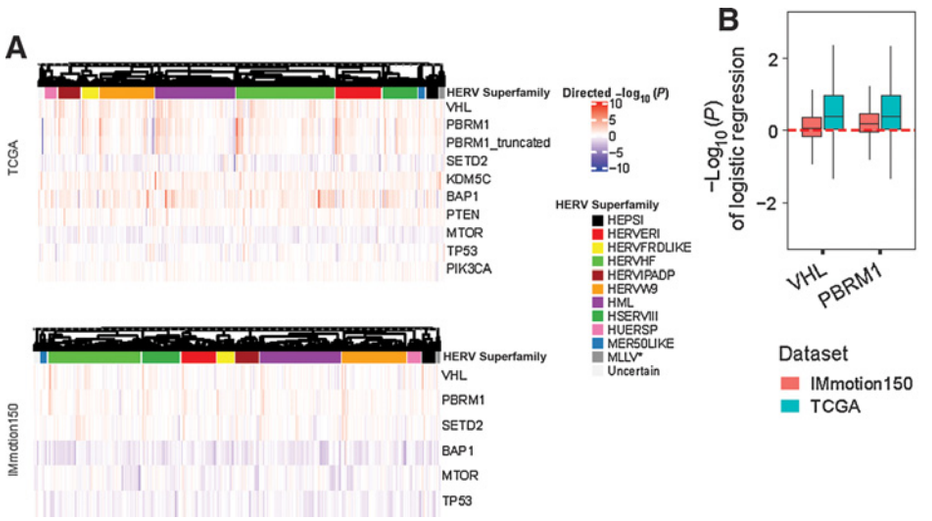

Figure 1.

ERVs are consistently upregulated in *VHL*- and *PBRM1*-mutant tumors. **A,** Logistic regression between indicated gene mutation status and individual hERV expression. Columns represent individual hERVs and rows are significantly mutated genes. Red indicates positive coefficient and blue indicates negative coefficient. **B,** Logistic regression *P* values of individual hERV expression in *VHL*- and *PBRM1*-mutant ccRCC.

and 92% of the detected hERVs shared in the TCGA and IMmotion150 datasets, respectively (Supplementary Fig. S1C). Of the 9 significantly mutated genes detected in the TCGA study, the IMmotion150 dataset contained mutational analysis of 6 (*PBRM1*, *VHL*, *SETD2*, *BAP1*, *MTOR*, *TP53*). We found that mutations in *VHL*, *PBRM1*, and *SETD2* were positively associated with hERV expression (**Fig. 1A**). Therefore, across both datasets, only *PBRM1* and *VHL* demonstrated a consistent positive association between mutation status and hERV expression (**Fig. 1B**; Supplementary Fig. S1D). These data suggest that both VHL and PBRM1 function to suppress hERV expression.

We then asked whether the association between *PBRM1* mutation and hERV expression was tissue-specific. We tested for the association of *PBRM1* mutations and hERV expression in non-KIRC TCGA cancers with a greater than 5% *PBRM1* alteration frequency and where hERV expression data was available (ref. 15; UCEC, CHOL, SKCM, MESO, and BLCA; Supplementary Fig. S2A). A consistent association between hERV expression and *PBRM1* mutation (Supplementary Fig. S2B–S2D) was not identified. These data demonstrate that the regulation of hERV expression by PBRM1 is unique to ccRCC.

PBRM1 downregulates hERVs of the HERVERI superfamily

Although the taxonomy of hERVs remains to be standardized, a commonly used classification system assigns hERVs to 11 superfamilies (23). We hypothesized that *PBRM1* inactivation may activate a specific subset of hERVs. We found that among hERVs that were upregulated in *PBRM1*-mutant tumors in both the TCGA and IMmotion150 datasets [generalized linear model (GLM) coefficiency>0, $P < 0.05$], the HERVERI superfamily was significantly enriched (**Fig. 2A** and **B**; Supplementary Fig. S3A). This enrichment was also seen when analyzing solely *PBRM1* LOF mutations (χ^2 $P =$ 2.645e-16, Supplementary Fig. S3A) in the TCGA KIRC dataset. The available IMmotion150 dataset regrettably does not include specifics about nucleotide or protein changes.

To validate that PBRM1 was functionally regulating hERV expression in a cell-autonomous manner, we silenced *PBRM1* in the UMRC2 RCC cell line (Supplementary Fig. S4A) and assessed changes in hERV expression by RNA-seq. Differential expression analysis demonstrated that *PBRM1* KD led to a change in a number of hERVs ($\log_2$-FC>0 and FDR $P < 0.05$; **Fig. 2C**) and that the number of upregulated hERVs were significantly enriched in the HERVERI superfamily (**Fig. 2D**). Similar enrichment of increasing expression of HERVERI superfamily of hERVs was also detected when we analyzed published transcriptome data from isogenic PBRM1-intact and -deficient A704 ccRCC cells (Supplementary Fig. S4B; ref. 21). These findings in aggregate indicate that PBRM1 functionally and selectively regulates HERVERI expression in a cell-autonomous manner.

PBRM1 inactivation promotes HERVERI family expression in a HIF-dependent manner

Because prior studies have demonstrated that PBRM1 inactivation amplifies HIF transcriptional activity (21) and that expression of HERV-E, a member of the HERVERI superfamily, is regulated in a HIF2α-dependent manner (24), we asked whether HIF1α and HIF2α were necessary for upregulation of HERVs following *PBRM1* KD. To this end, we performed RNA-seq and HERV quantification after knockdown of *HIF1A* and *HIF2A* in the previously generated UMRC2-shPBRM1 cells (Supplementary Fig. S4A). A large portion of HERVs upregulated upon PBRM1 KD were downregulated by silencing of either HIF1α or HIF2α (**Fig. 3A** and **B**). Furthermore, HIF1α and HIF2α regulated the expression of a relatively similar set of hERVs upregulated upon *PBRM1* KD (Supplementary Fig. S5) and to a similar degree (**Fig. 3C**). Restricting the analysis to only the HERVERI superfamily of hERVs demonstrated comparable findings (**Fig. 3D–F**). Nonetheless, there were hERVs upregulated upon *PBRM1* KD that were not altered by *HIF1A* or *HIF2A* siRNA (Supplementary Fig. S5), suggesting that PBRM1 might regulate these hERVs through HIF-independent processes, such as solely through nucleosome repositioning. In aggregate, these results indicate that both HIF1α and HIF2α are necessary for the expression of a large proportion of hERVs downregulated by PBRM1.

Discussion

hERV expression has been associated with both prognosis and ICB response in ccRCC (14, 15). To understand the underlying mechanism of hERV regulation in ccRCC, we asked whether genes mutated in ccRCC could influence hERV transcription. Herein we report that PBRM1 loss is associated with increased hERV expression, particularly the HERVERI superfamily. PRBM1's regulation of hERVs is specific to ccRCC and not seen in other TCGA tumor types. Moreover, we demonstrate that PBRM1 inactivation alters hERV expression in a

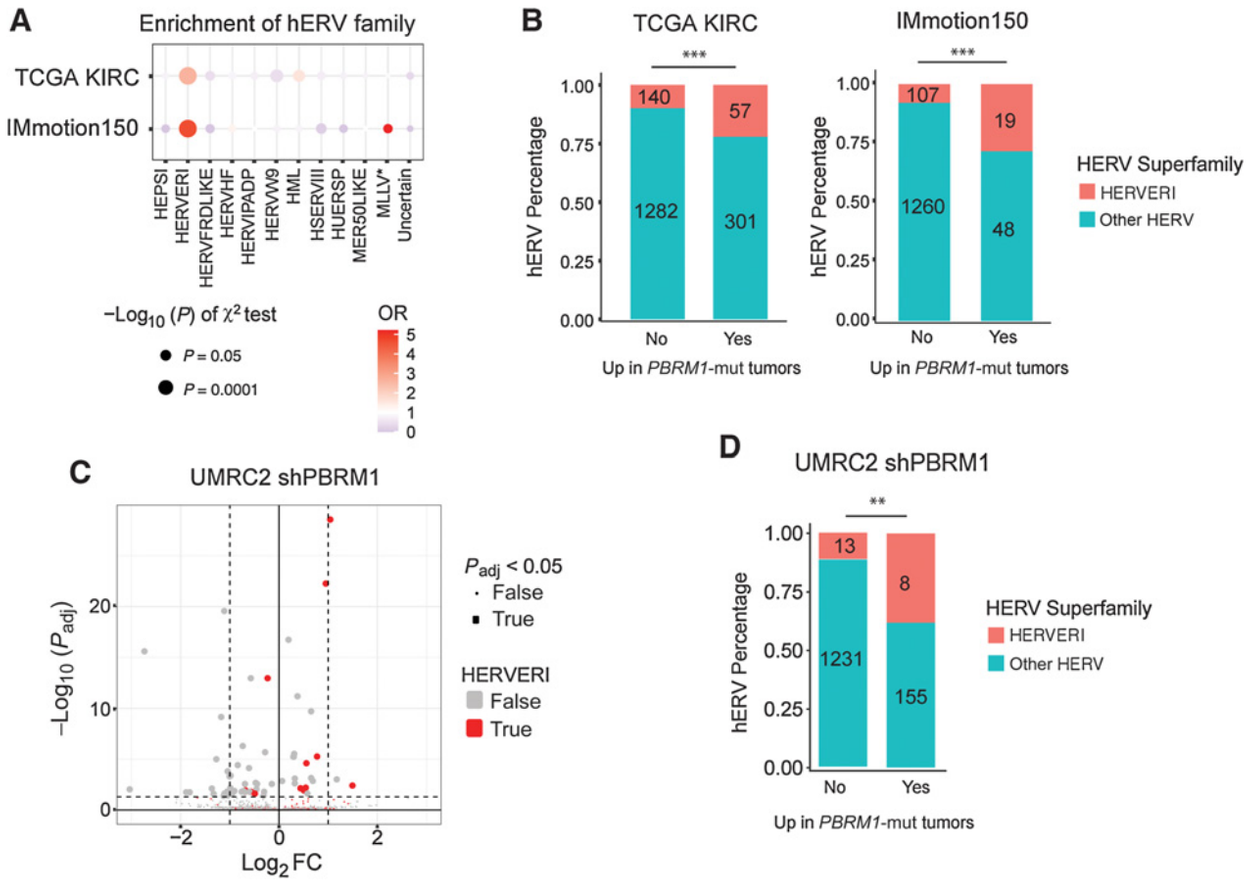

Figure 2.

PBRM1 downregulates hERVs of the HERVERI superfamily. **A,** $-\text{Log}_{10}$ *P* value (circle size) and the OR (color) of the χ^2 test of HERVERI enrichment in *PBRM1*-mutated tumors in TCGA and IMmotion150. **B,** Percentage of HERVERI versus other hERVs upregulated (YES) or not upregulated (NO) in *PBRM1*-mutant TCGA and IMmotion150 tumors. ***, χ^2 test $P < 0.001$. Number of the hERVs in each group are indicated in the bars. **C,** Differentially expressed hERVs in *PBRM1* KD versus. WT UMRC2 cells. Red dots indicate hERVs of the HERVERI family. Larger points indicate Benjamini–Hochberg P_{adj} <0.05. **D,** Percentage of HERVERI hERVs upregulated (YES) or not upregulated (NO) in shPBRM1 versus empty vector control (shNS) UMRC2 cells. ***, χ^2 test $P < 0.001$.

cell-autonomous manner and that both HIF1α and HIF2α are necessary for upregulation of PBRM1-dependent hERVs.

Our study offers a potential explanation for the well-established observation that *PBRM1* mutations are associated with a better prognosis relative to *SETD2*- and *BAP1*-mutant tumors, as well as the variably reported observation that *PBRM1* mutations are associated with enhanced ICB response in ccRCC (5–7, 11, 20, 25–27). Because *PBRM1* mutations appear to be an early event in ccRCC pathogenesis, often occurring as a truncal mutation (28), it is possible that the development of a PBRM1-deficient tumor necessitates a balance between immune surveillance and immune escape against highly immunogenic hERVs or through robust immune checkpoint upregulation and T-cell exhaustion. The addition of ICB could disrupt this balance to provoke a robust adaptive immune response, stimulating primed, anti-hERV T cells, resulting in favorable clinical outcomes. Indeed, prior work by Childs and colleagues supports this notion, as they saw an increase in HERVE tetramer–positive T cells in responding ccRCC patients following allogeneic stem cell transplant (29).

Choueiri and colleagues looked for association between SWI/SNF alterations and ICB response in two large datasets of ICB-treated solid tumor types ($n = 7$) (11) and saw that, in aggregate, mutations in SWI/SNF complex members did not associate with time to treatment failure (TTF) or overall survival (OS) in the cohort as a whole (11). However, when limiting the analysis to patients with ccRCC, tumors with SWI/SNF mutations showed significantly improved TTF and OS, an effect driven primarily by *PBRM1* mutations. These results suggest that the combination of *PBRM1* mutations and the genetics underlying ccRCC result in a unique phenotype. Our demonstration that PBRM1 regulates hERVs in a manner dependent on both HIF1α and HIF2α may explain this link, as the loss of VHL results in constitutively stabilized HIFα and HIF transcriptional activity, and VHL mutations are unique to ccRCC development. Our data demonstrate that tumors with dual inactivation of VHL and PBRM1, as expected, appear to have elevated hERV expression, and this may explain the consistent finding that *PBRM1* mutations associate with improved ICB outcomes only in ccRCC.

It is interesting that mutations in other PBAF complex members unique to the PBAF complex (ARID2 and BRD7) are associated with improved clinical outcomes to ICB treatment in *NRAS*-mutant melanoma, even when controlled for tumor mutational burden, tumor purity, and treatment (30). Furthermore, PBRM1, ARID2, and BRD7

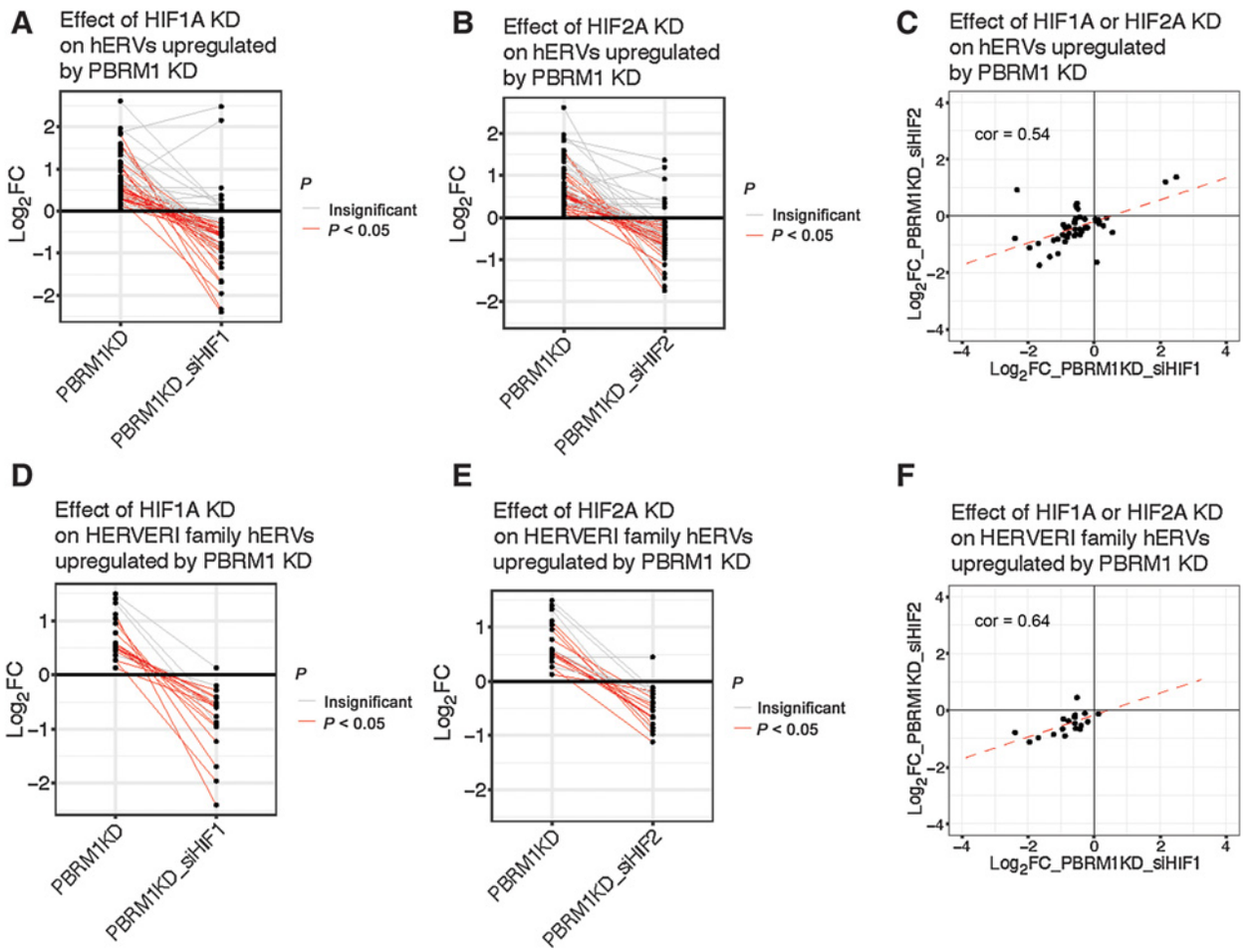

Figure 3.

PBRM1 inactivation promotes HERVERI family expression in a HIF-dependent manner. **A,** Log_2 fold change of hERVs upregulated by *PBRM1* KD in UMRC2 PBRM1-KD and UMRC2 PBRM1-KD_siHIF1 cells. **B,** Log_2 fold change of hERVs upregulated by *PBRM1* KD in UMRC2 PBRM1-KD and UMRC2 PBRM1-KD_siHIF2 cells. **C,** Log_2 fold change of hERVs in UMRC2 PBRM1-KD_siHIF1 cells versus PBRM1-KD_siHIF2 cells. Pearson correlation of the log_2 fold changes is labeled in the plot. Only hERVs upregulated by *PBRM1* KD in UMRC2 cells are shown. **D,** Log_2 fold change of HERVERI family hERVs upregulated by *PBRM1* KD in UMRC2 PBRM1-KD and UMRC2 PBRM1-KD_siHIF1 cells. **E,** Log_2 fold change of HERVERI family hERVs upregulated by *PBRM1* KD in UMRC2 PBRM1-KD and UMRC2 PBRM1-KD_siHIF2 cells. **F,** Log_2 fold change of HERVERI family hERVs in UMRC2 PBRM1-KD_siHIF1 cells versus PBRM1-KD_siHIF2 cells. Pearson correlation of the log_2 fold changes is labeled in the plot. Only HERVERI family hERVs upregulated by *PBRM1* KD in UMRC2 cells are shown.

were found to be tumor cell–autonomous regulators of T-cell killing in murine melanoma cell lines (26). Along these lines, we had previously described a key role for HIF1A and HIF2A in *BRAF*-mutant melanoma, which, like ccRCC, is highly angiogenic (31). In addition, recently published work demonstrates that SETDB1 is a key H3K9 methyltransferase that is critical for silencing of transposable elements including hERVs (32, 33). In aggregate, these data suggest key roles for both nucleosome positioning and modification of histone tails in the repression of hERV expression and strongly argues for a special interaction between the PBAF complex and HIF in mediating ICB response.

PBRM1 inactivation has been shown to amplify HIF transcriptional activity and is therefore associated with higher angiogenic signaling (7, 21). This increased HIF activity and subsequent VEGF production might account for the inconsistent association of *PBRM1* mutations with ICB benefit in ccRCC. VEGF is known to be highly immunosuppressive by preventing dendritic cell maturation, and the combination of VEGF inhibition and ICB has been successful in ccRCC. It is therefore notable that the absence of an association between *PBRM1* mutation and ICB response in the IMmotion150, IMmotion151, and JAVELIN Renal 101 were all in the first line setting (8, 9, 20), where tumors have not had significant exposure to VEGF blockade.

Our work shows that PBRM1-regulated hERVs in both tumors and UMRC2 cells are enriched in the ERVERI superfamily. What mediates the selective upregulation of HERVERI hERVs remains unknown. Furthermore, although either HIF1α and HIF2α are necessary for upregulation of HERVERI hERVs, we do not know whether this represents a direct or indirect consequence of HIF activation. Finally, although we propose a model whereby upregulated hERV expression serves as a tumor-associated antigen in ccRCC, definitive evidence that ERVs serve as the primary tumor-associated antigens driving ICB response is still lacking. Future studies should focus on validation of our results in other model systems, as well as understanding additional modifiers of ICB response in PBRM1-deficient ccRCC.

Authors' Disclosures

I.J. Davis reports grants from NIH during the conduct of the study, as well as other support from Triangle Biotechnology, Inc. outside the submitted work. W.Y. Kim reports grants from NIH, AACR Kure It, Kidney Cancer Association, and University Cancer Research Fund during the conduct of the study; stock and other ownership interests in AbbVie, Abbott, Amgen, Arvinas, BeiGene, Bluebird Bio, Bristol Myers Squibb, Myovant, Natera, Oramed, Zentalis, and ACT (Advanced Chemotherapy Technologies); and research funding from Acerta, GeneCentric, and Merck. No disclosures were reported by the other authors.

Authors' Contributions

M. Zhou: Data curation, formal analysis, validation, visualization, writing–original draft, writing–review and editing. **J.Y. Leung:** Formal analysis, investigation, writing–original draft. **K.H. Gessner:** Data curation, investigation. **A.J. Hepperla:** Formal analysis, investigation, writing–review and editing. **J.M. Simon:** Formal analysis, investigation, writing–review and editing. **I.J. Davis:** Supervision, investigation, writing–review and editing. **W.Y. Kim:** Conceptualization, supervision, writing–original draft, writing–review and editing.

Acknowledgments

We acknowledge the members of the Kim Lab for useful discussions. This work was supported by NIH R01 CA202053 (to W.Y. Kim); 2012 AACR-Kure It Grant for Kidney Cancer Research, grant number 12-60-36-KIM (to W.Y. Kim); the Kidney Cancer Association (to W.Y. Kim); and the University Cancer Research Fund (UCRF).

Received June 17, 2021; revised November 5, 2021; accepted January 5, 2022; published first January 10, 2022.

References

1. Siegel RL, Miller KD, Fuchs HE, Jemal A. Cancer statistics, 2021. CA Cancer J Clin 2021;71:7–33.
2. The Cancer Genome Atlas Research Network. Comprehensive molecular characterization of clear cell renal cell carcinoma. Nature 2013; 499:43–9.
3. Varela I, Tarpey P, Raine K, Huang D, Ong CK, Stephens P, et al. Exome sequencing identifies frequent mutation of the SWI/SNF complex gene PBRM1 in renal carcinoma. Nature 2011;469:539–42.
4. Wilson BG, Roberts CWM. SWI/SNF nucleosome remodellers and cancer. Nat Rev Cancer 2011;11:481–92.
5. Braun DA, Ishii Y, Walsh AM, Allen EMV, Wu CJ, Shukla SA, et al. Clinical validation of PBRM1 alterations as a marker of immune checkpoint inhibitor response in renal cell carcinoma. JAMA Oncol 2019;5:1631–3.
6. Miao D, Margolis CA, Gao W, Voss MH, Li W, Martini DJ, et al. Genomic correlates of response to immune checkpoint therapies in clear cell renal cell carcinoma. Science 2018;359:801–6.
7. Braun DA, Hou Y, Bakouny Z, Ficial M, Angelo MS, Forman J, et al. Interplay of somatic alterations and immune infiltration modulates response to PD-1 blockade in advanced clear cell renal cell carcinoma. Nat Med 2020;26:909–18.
8. Motzer RJ, Robbins PB, Powles T, Albiges L, Haanen JB, Larkin J, et al. Avelumab plus axitinib versus sunitinib in advanced renal cell carcinoma: biomarker analysis of the phase 3 JAVELIN Renal 101 trial. Nat Med 2020;26: 1733–41.
9. Motzer RJ, Banchereau R, Hamidi H, Powles T, McDermott D, Atkins MB, et al. Molecular subsets in renal cancer determine outcome to checkpoint and angiogenesis blockade. Cancer Cell 2020;38:803–17.
10. Conway J, Taylor-Weiner A, Braun D, Bakouny Z, Choueiri TK, Van Allen EM. PBRM1 loss-of-function mutations and response to immune checkpoint blockade in clear cell renal cell carcinoma. Medrxiv 2020.10.30.20222356 [Preprint]. 2020. Available from: https://doi.org/10.1101/2020.10.30.20222356.
11. Alaiwi SA, Nassar AH, Xie W, Bakouny Z, Berchuck JE, Braun DA, et al. Mammalian SWI/SNF complex genomic alterations and immune checkpoint blockade in solid tumors. Cancer Immunol Res 2020;8:1075–84.
12. Bannert N, Kurth R. The evolutionary dynamics of human endogenous retroviral families. Ann Rev Genom Hum G 2006;7:149–73.
13. Lander ES, Linton LM, Birren B, Nusbaum C, Zody MC, Baldwin J, et al. Initial sequencing and analysis of the human genome. Nature 2001;409:860–921.
14. de Cubas AA, Dunker W, Zaninovich A, Hongo RA, Bhatia A, Panda A, et al. DNA hypomethylation promotes transposable element expression and activation of immune signaling in renal cell cancer. JCI Insight 2020;5: e137569.
15. Smith CC, Beckermann KE, Bortone DS, de Cubas AA, Bixby LM, Lee SJ, et al. Endogenous retroviral signatures predict immunotherapy response in clear cell renal cell carcinoma. J Clin Invest 2018;128:4804–20.
16. Wang-Johanning F, Frost AR, Johanning GL, Khazaeli MB, LoBuglio AF, Shaw DR, et al. Expression of human endogenous retrovirus k envelope transcripts in human breast cancer. Clin Cancer Res 2001;7:1553–60.
17. Büscher K, Trefzer U, Hofmann M, Sterry W, Kurth R, Denner J. Expression of human endogenous retrovirus K in melanomas and melanoma cell lines. Cancer Res 2005;65:4172–80.
18. Florl AR, Löwer R, Schmitz-Dräger BJ, Schulz WA. DNA methylation and expression of LINE-1 and HERV-K provirus sequences in urothelial and renal cell carcinomas. Br J Cancer 1999;80:1312–21.
19. Panda A, de Cubas AA, Stein M, Riedlinger G, Kra J, Mayer T, et al. Endogenous retrovirus expression is associated with response to immune checkpoint blockade in clear cell renal cell carcinoma. JCI insight 2018;3: e121522.
20. McDermott DF, Huseni MA, Atkins MB, Motzer RJ, Rini BI, Escudier B, et al. Clinical activity and molecular correlates of response to atezolizumab alone or in combination with bevacizumab versus sunitinib in renal cell carcinoma. Nat Med 2018;24:749–57.
21. Gao W, Li W, Xiao T, Liu XS, Kaelin WG. Inactivation of the PBRM1 tumor suppressor gene amplifies the HIF-response in VHL−/− clear cell renal carcinoma. Proc Natl Acad Sci U S A 2017;114:1027–32.
22. Yoshihara K, Shahmoradgoli M, Martínez E, Vegesna R, Kim H, Torres-Garcia W, et al. Inferring tumour purity and stromal and immune cell admixture from expression data. Nat Commun 2013;4:2612.
23. Vargiu L, Rodriguez-Tomé P, Sperber GO, Cadeddu M, Grandi N, Blikstad V, et al. Classification and characterization of human endogenous retroviruses; mosaic forms are common. Retrovirology 2016;13:7.
24. Cherkasova E, Weisman Q, Childs RW. Endogenous retroviruses as targets for antitumor immunity in renal cell cancer and other tumors. Front Oncol 2013;3:243.
25. Kapur P, Peña-Llopis S, Christie A, Zhrebker L, Pavía-Jiménez A, Rathmell WK, et al. Effects on survival of BAP1 and PBRM1 mutations in sporadic clear-cell renal-cell carcinoma: a retrospective analysis with independent validation. Lancet Oncol 2013;14:159–67.
26. Pan D, Kobayashi A, Jiang P, de Andrade LF, Tay RE, Luoma A, et al. A major chromatin regulator determines resistance of tumor cells to T cell–mediated killing. Science 2018;359:770–5.
27. Keenan TE, Burke KP, Allen EMV. Genomic correlates of response to immune checkpoint blockade. Nat Med 2019;25:389–402.
28. Turajlic S, Xu H, Litchfield K, Rowan A, Horswell S, Chambers T, et al. Deterministic evolutionary trajectories influence primary tumor growth: TRACERx Renal. Cell 2018;173:595–610.
29. Takahashi Y, Harashima N, Kajigaya S, Yokoyama H, Cherkasova E, McCoy JP, et al. Regression of human kidney cancer following allogeneic stem cell transplantation is associated with recognition of an HERV-E antigen by T cells. J Clin Invest 2008;118:1099–109.
30. Conway JR, Dietlein F, Taylor-Weiner A, AlDubayan S, Vokes N, Keenan T, et al. Integrated molecular drivers coordinate biological and clinical states in melanoma. Nat Genet 2020;52:1373–83.
31. Hanna SC, Krishnan B, Bailey ST, Moschos SJ, Kuan P-F, Shimamura T, et al. HIF1α and HIF2α independently activate SRC to promote melanoma metastases. J Clin Invest 2013;123:2078–93.
32. Griffin GK, Wu J, Iracheta-Vellve A, Patti JC, Hsu J, Davis T, et al. Epigenetic silencing by SETDB1 suppresses tumour intrinsic immunogenicity. Nature 2021; 595:309–14.
33. Zhang S-M, Cai WL, Liu X, Thakral D, Luo J, Chan LH, et al. KDM5B promotes immune evasion by recruiting SETDB1 to silence retroelements. Nature 2021; 598:682–7.